

University of Groningen

## Molecular dynamics simulation of a charged biological membrane

López Cascales, J. J.; García de la Torre, J.; Marrink, S. J.; Berendsen, H. J. C.

*Published in:*  
Journal of Chemical Physics

*DOI:*  
[10.1063/1.470992](https://doi.org/10.1063/1.470992)

**IMPORTANT NOTE: You are advised to consult the publisher's version (publisher's PDF) if you wish to cite from it. Please check the document version below.**

*Document Version*  
Publisher's PDF, also known as Version of record

*Publication date:*  
1996

[Link to publication in University of Groningen/UMCG research database](#)

*Citation for published version (APA):*

López Cascales, J. J., García de la Torre, J., Marrink, S. J., & Berendsen, H. J. C. (1996). Molecular dynamics simulation of a charged biological membrane. *Journal of Chemical Physics*, 104(7), 2713 - 2720. <https://doi.org/10.1063/1.470992>

**Copyright**

Other than for strictly personal use, it is not permitted to download or to forward/distribute the text or part of it without the consent of the author(s) and/or copyright holder(s), unless the work is under an open content license (like Creative Commons).

The publication may also be distributed here under the terms of Article 25fa of the Dutch Copyright Act, indicated by the "Taverne" license. More information can be found on the University of Groningen website: <https://www.rug.nl/library/open-access/self-archiving-pure/taverne-amendment>.

**Take-down policy**

If you believe that this document breaches copyright please contact us providing details, and we will remove access to the work immediately and investigate your claim.

*Downloaded from the University of Groningen/UMCG research database (Pure): <http://www.rug.nl/research/portal>. For technical reasons the number of authors shown on this cover page is limited to 10 maximum.*

# Molecular dynamics simulation of a charged biological membrane

J. J. López Cascales

*Departamento de Química Física, Facultad de Ciencias, Universidad de Murcia, Campus de Espinardo, 30071 Murcia, Spain and BIOSON Institute, Department of Biophysical Chemistry, University of Groningen, Nijenborgh 4, 9747AG Groningen, The Netherlands*

J. García de la Torre<sup>a)</sup>

*Departamento de Química Física, Facultad de Ciencias, Universidad de Murcia, Campus de Espinardo, 30071 Murcia, Spain*

S. J. Marrink and H. J. C. Berendsen

*BIOSON Institute, Department of Biophysical Chemistry, University of Groningen, Nijenborgh 4, 9747AG Groningen, The Netherlands*

(Received 18 July 1995; accepted 2 November 1995)

A molecular dynamics simulation of a membrane with net charge in its liquid-crystalline state was carried out. It was modeled by dipalmitoylphosphatidylserine lipids with net charge, sodium ions as counterions and water molecules. The behavior of this membrane differs from that was shown by other membranes without a net charge as a consequence of strong Coulomb interaction between atoms of adjacent phospholipids. The most remarkable effect produced by such interaction between neighboring lipids is a reduction of the surface area per phospholipid compared to an uncharged membrane. In addition, other properties of the membrane were also affected by this interaction between adjacent lipids such as the atom distribution across the membrane, the diffusion coefficient of the different components of the membrane and the order parameter of the phospholipid hydrocarbon region. Some comparisons of this membrane with dipalmitoylphosphatidylcholine membrane without net charge at similar conditions are presented. © 1996 American Institute of Physics. [S0021-9606(96)50606-X]

## I. INTRODUCTION

Phospholipids play an important role in the control of diffusion of water and ions across cellular membranes. In general, the membrane involves a broad variety of phospholipids; while each one plays a different role in the diffusion of ions and small molecules across the membranes, they also provide the required environment for proteins embedded in the membrane.

The phosphatidylserine lipids (PS) are constituents of the membranes of eukaryotic cells with a molar fraction of roughly 7%. They are the most important negatively charged phospholipids under physiological conditions, playing an important role in the cells of the central nervous system, supposedly contributing to the manic depressive illness as a consequence of some structural changes associated with the presence of different concentrations of ions.<sup>1</sup> In spite of this, much less data are available in the literature for this phospholipid than for phosphatidylcholine (PC) or phosphatidylethanolamine (PE).

At neutral pH, where the PS has a net negative charge, saturated species of PS exhibit gel to liquid-crystal transition temperatures<sup>2</sup> which are higher than for the corresponding PC but lower than for the corresponding PE. No pretransition is observed. The phase transition temperature can be changed by about 20 degrees by changes in the ionic composition of the aqueous phase.<sup>3</sup> X-ray and spectroscopic data<sup>1,4,5</sup> indicate

that at neutral pH aqueous dispersions of saturated and unsaturated PS adopt a lamellar phase.

Computer simulation is a powerful tool that provides a detailed information on the dynamic and static behavior of phospholipids in a membranes. Thus, for example, Pastor<sup>6</sup> used a Brownian dynamics simulation of a lipid chain for modeling motional properties of a dipalmitoylphosphatidylcholine (DPPC) bilayer. De Loof<sup>7</sup> performed computer simulations of a membrane of DPPC by using a combined approach of molecular and stochastic dynamics and a mean field based on a Marčelja model.<sup>8</sup> In any of the simulations mentioned above, no water molecules were taken into account in an explicit manner. Venable<sup>9</sup> carried out a molecular dynamics (MD) simulation of a fluid-phase DPPC lipid bilayer. Several MD simulations of a model of DLPE (dilauroylphosphatidylethanolamine) bilayer have been performed;<sup>10-13</sup> palmitoyloleoylphosphatidylcholine (POPC) was studied by Heller *et al.*<sup>14</sup> In the latter full atomic detail was taken into account in the simulation, including water molecules.

Previous investigations in this laboratory<sup>15-18</sup> have been concerned with MD simulations of uncharged membranes with full atomic detail. Here, we employ the same methodology in a MD simulation of a charged membrane of dipalmitoylphosphatidylserine (DPPS) in its liquid-crystalline state ( $L_{\alpha}$ ), with the aim of finding out the role played by phospholipids bearing a net charged in a biological membrane. We will compare the results emerged from this simulation with experimental and other simulation data, in particular with those of a membrane of DPPC.

<sup>a)</sup>To whom correspondence should be addressed.

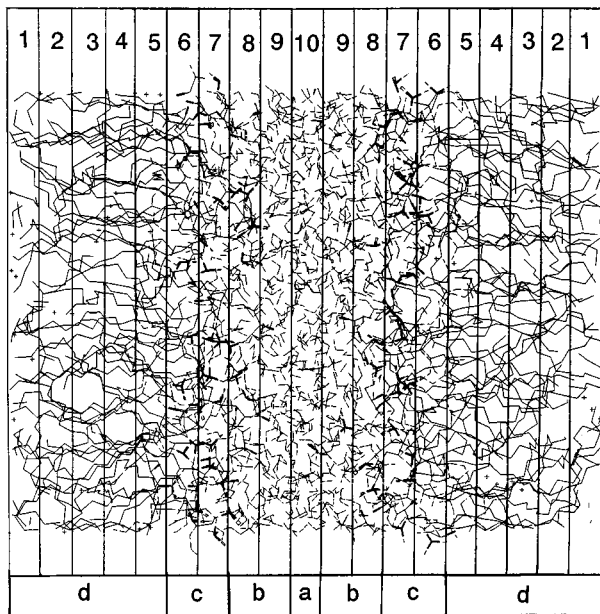


FIG. 1. A snapshot of the membrane model during the simulation, showing the 10 slabs of 0.3 nm of thickness which were used for analysis. Four different regions can also be observed: (a) Bulk water, (b) interface water-DPPS, (c) serine+phosphate, (d) hydrocarbon tails.

## II. METHOD AND MODELS

### A. Setting up the membrane model

One molecule of DPPS was generated with the commercial package HYPERCHEM<sup>19</sup> (employing its build molecule utility) and it was randomly rotated and copied 32 times on two layers. The empty volume between these two monolayers of 1 nm thickness was filled up with 796 water molecules of the SPC<sup>20</sup> (single point charge) model. As DPPS at physiological conditions carries a negative net charge, sodium ions were used as counterions and 64 initial water molecules were substituted by 64 ions following a minimum energy criteria. Except for the water molecules a united atom model was used. At the end, the membrane model consisted of 64 DPPS<sup>-</sup>, 64 Na<sup>+</sup> and 732 H<sub>2</sub>O, which amounts to a total number of atoms of 5460. A snapshot of this membrane model is shown in Fig. 1.

Table I displays the charge distribution on each DPPS atom, following the atom numeration of Fig. 2. The computation was carried out using the quantum mechanical CNDO<sup>21</sup> method (complete neglect of differential overlap). The atom charges that were employed in our simulations (included sodium ions) were equal to the values given in Table I, divided by a factor of 2 (except for the SPC model). This has turned out to be effective in the simulation of a soap/alcohol/water system<sup>17</sup> and in the simulation of a micelle<sup>22</sup> as well. The physical justification for this reparameterization is, in short, that the coulombic interactions in the system are exaggerated due to an insufficient screening performance of the SPC water molecules by the absence of polarizability and induced dipoles in the model.

TABLE I. Charge on each atom of a molecule of DPPS<sup>-</sup>, sodium ions Na<sup>+</sup> and water. During the simulation all charges were divided by 2, except for the water molecules.

Molecule	Num. atom.	Atom type	Charge ( <i>e</i> )
DPPS	1	NH <sub>3</sub> <sup>+</sup>	0.6086
DPPS	2	CH	0.1377
DPPS	3	C	0.2941
DPPS	4	O	-0.5645
DPPS	5	O	-0.5645
DPPS	6	CH <sub>2</sub>	0.1011
DPPS	7	O	-0.3648
DPPS	8	P	1.0888
DPPS	9	O	-0.7094
DPPS	10	O	-0.7094
DPPS	11	O	-0.3907
DPPS	12	CH <sub>2</sub>	0.0726
DPPS	13	CH	0.2000
DPPS	14	O	-0.3599
DPPS	15	C	0.5399
DPPS	16	O	-0.3792
DPPS	17-31	CH <sub>2</sub> -CH <sub>3</sub>	0.0000
DPPS	32	CH <sub>2</sub>	0.2000
DPPS	33	O	-0.3599
DPPS	34	C	0.5399
DPPS	35	O	-0.3793
DPPS	36-50	CH <sub>2</sub> -CH <sub>3</sub>	0.0000
Ion		Na <sup>+</sup>	1.0000
Water		HW	-0.820
Water		OW	0.410

### B. Starting up the simulation

Periodic boundary conditions were applied along the three space dimensions. With the aim of maintaining the temperature constant along the simulation, the whole system was weakly coupled to a temperature bath<sup>23</sup> of 350 K with a coupling (or dumping) constant  $\tau_T$  of 0.1 ps. This temperature was selected such that it was above the DPPS<sup>-</sup> transition temperature<sup>4,24</sup> of 326 K. In a similar way, the pressure

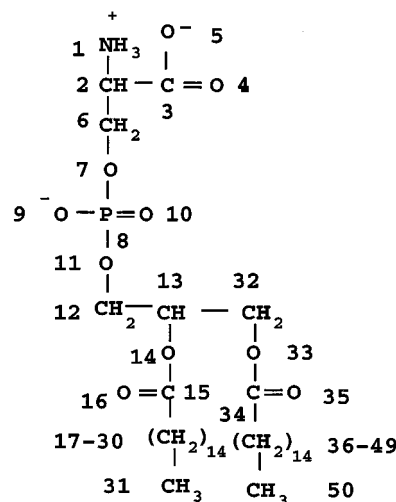


FIG. 2. Atom numbering of a molecule of dipalmitoylphosphatidylserine (DPPS).

was maintained constant by anisotropic coupling to a reference pressure<sup>23</sup> of 1 atm with a dumping constant  $\tau_p$  of 0.5 ps.

The GROMOS force field<sup>25,26</sup> was used in our simulations. The dihedral potential and the Lennard-Jones interactions of the hydrocarbon tail groups were changed to the Ryckaert and Bellemans form<sup>27</sup> as has already been explained in previous articles.<sup>15,18,28</sup> The Lennard-Jones parameters as well as the 1–4 interaction parameters of Ryckaert–Bellemans potential were shown in a previous article.<sup>18</sup> A constant simulation time step of 2 fs was applied during the whole of the simulation.

As electrostatic interactions play an important role in the dynamics of molecules with net charge (sodium ions and DPPS) or with a permanent dipole moment (water molecules), two different cutoff radii were utilized in our simulations, a spherical short cutoff of 0.75 nm and a cylindrical long one of 1.7 nm analogous to previous simulations of DPPC.<sup>15,18,28</sup>

After the membrane model was built up, we applied a steepest descent energy minimization procedure with the goal of reducing the high potential energy before starting the MD simulations. After this procedure, the box edges reached the values of  $x_0=4.61$ ,  $y_0=4.26$ , and  $z_0=5.08$  nm, where  $x$  and  $y$  are the axes of the membrane plane. The next step was to equilibrate the cell dimensions and the total energy of the system. A computational trick was employed for the acceleration of such equilibration: the masses of the hydrogens were increased to 16. This increase of the hydrogen mass slowed down the faster rotational motions of the water molecules by a factor of 4 and it allowed us to increase the time step with a factor of 4, reaching 8 fs. A simulation under these conditions was performed for 200 ps. Afterwards, the hydrogen masses were reduced again to their original value of 1 and another simulation for 160 ps was performed. Then, after a total trajectory length of 360 ps of simulation, the box dimensions equilibrated at the values of  $x=4.36$ ,  $y=4.09$  and  $z=5.6$  nm, with a potential energy of  $-0.36 \times 10^5$  kJ/mol. Finally, a MD run of 184 ps length was carried out. The results shown below were obtained from the trajectory of this run.

### III. RESULTS AND DISCUSSION

#### A. Surface area per phospholipid and radial distribution of head groups

The mean surface area per phospholipid was of 0.54 nm<sup>2</sup>, which agrees with the experimental results for DPPS in its liquid crystalline state,<sup>24,29,30</sup> where values in the range from 0.50 to 0.55 nm<sup>2</sup> have been measured.

It is pertinent to point out the surface anisotropy that we found in the computing box, where the  $x$  length is roughly 10% longer than the  $y$  length, contrary to what one would expect from a disordered fluid system. The origin of this feature will be presented and discussed below.

A comparison between experimental and simulated data on the DPPS and the DPPC surface area (DPPC being a neutral phospholipid at physiological conditions with surface

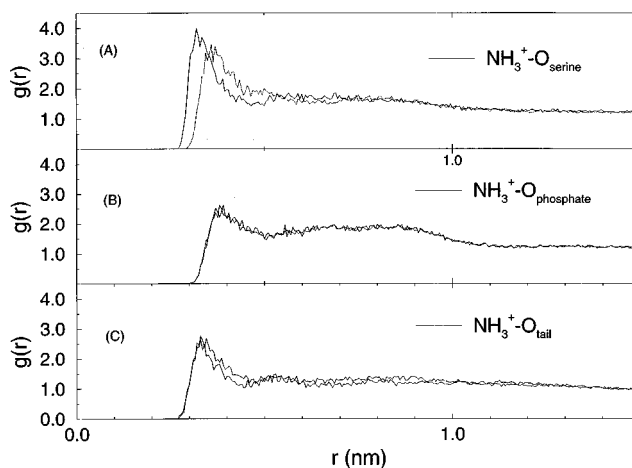


FIG. 3. Intermolecular radial distribution function of oxygens surrounding ammonium nitrogen group. (a) Serine nitrogen and serine oxygens 4,5. (b) Serine nitrogen and phosphate oxygens 9,10. (c) Serine nitrogen and carboxyl oxygen tail 16,34.

area of 0.6 nm<sup>2</sup>), reveals an interesting difference: the DPPC area is 10% larger than the DPPS area. This is in contrast with the expectation of a larger area for DPPS compared with the DPPC due to the coulombic repulsive interactions between neighboring phospholipids.

Previous investigations<sup>31,32</sup> have already suggested the possibility of a charge interaction between the ammonium group (with positive net charge) and some oxygens (with negative net charge) of adjacent phospholipids. In order to investigate this point, the radial distribution functions  $g(r)$  of some atoms involved in potential intermolecular charge interactions were determined [Figs. 3(a), 3(b), and 3(c)]. Note that, due to the inhomogeneous density distribution in the system, the radial distribution functions decay to one only for long distances. The radial distribution function  $g(r)$  was defined by

$$g(r) = \frac{N(r)}{4\pi r^2 \rho \delta r}, \quad (1)$$

where  $N(r)$  is the number of oxygens in a spherical layer between  $r$  and  $r + \delta r$ ,  $r$  being the distance from the reference atom, and  $\rho$  is the number density taken as the ratio of the number of atoms to the volume of the computing box.

Figures 3(a), 3(b), and 3(c) show the presence of some peaks in the radial distribution between the ammonium nitrogen and different oxygen groups. From the area of the first neighbor peaks [up to the first minimum of  $g(r)$ ], we are able to obtain the coordination numbers of each kind of oxygen around the ammonium. The values that we find are 1.3, 1.0, and 1.0, for serine carbonyl, phosphate and tail carbonyl oxygen, respectively. From these results, we see that the ammonium group shows a strong intermolecular coordination which could lead to a decrease of the phospholipid surface area in DPPS. The ammonium group prefers to be bound to serine carbonyl oxygen rather than to phosphatidyl or carbonyl tail oxygens. Figure 3(a) also shows an apparent distinction between the two serine oxygens. This is a consequence

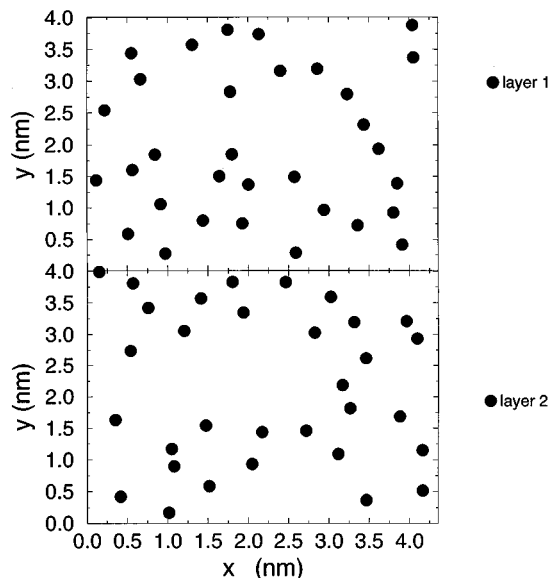


FIG. 4. Centers of mass of the serine+phosphate group on both layers of the membrane averaged over 10 ps of the simulated trajectory.

of insufficient sampling due to the finite trajectory length of our simulations, since these oxygens are chemically equivalent.

Figure 4 displays the lateral distribution of the center of mass of the phospholipid head groups on both layer planes, including the phosphate group in the calculation of the center of mass. From this, we see that the phospholipid heads tend to form a cluster as a consequence of the presence of the intermolecular charge interaction. This result is clearly different from the head distribution found for DPPC membranes,<sup>9,17,18</sup> where the phospholipid heads are uniformly spread on the membrane surface. This anisotropic distribution of the head groups explains the length difference between  $x$  and  $y$  of the cell edges. The anisotropy is an artifact of periodic boundary conditions and is not expected to occur in biological membranes. Moreover, DPPS is a component of the inside layer of the erythrocyte membrane with abundance of only 7%, in which extensive clustering is not expected to take place.

## B. Atom and charge distribution across the membrane

Figure 5 shows the atom distribution across the bilayer membrane for different atoms and groups of atoms from the center of a bilayer to the center of the next one.

From this, we see as the serine group distribution (referred to its center of mass) is fairly constrained in two sharp peaks with a width at halfheight of roughly 0.5 nm (interpreting the peaks as Gaussian distributions), compared with the broader distribution of the DPPC head<sup>16,18,31</sup> of 0.66 nm. In other words, the DPPS head distribution is sharper than the DPPC one. We conclude that the presence of charge interaction between adjacent DPPS molecules generates a more constrained structure than in the DPPC case, and as a result, a sharper peak for the head distribution is obtained.

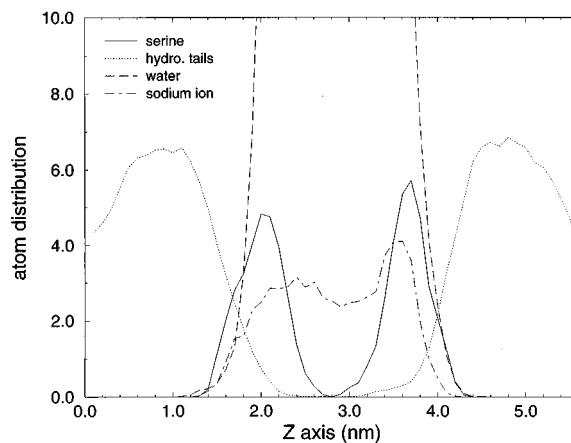


FIG. 5. Atom distribution across the membrane. In the serine and water case, the distribution is based on their center of mass.

During the simulation time, neither sodium ions nor water molecules dissolved into the membrane. If we look at Fig. 5, we see how the highly hydrophobic nature of the hydrocarbon region reduces the presence of charged species to practically zero in this region. Water and sodium can only penetrate into the interface zone which is mainly occupied by serine groups and not into the hydrocarbon region, as in the DPPC case.<sup>18,28</sup> Also the phosphate groups appear to be much less hydrated than in DPPC.

In the sodium distribution, the maximum concentration is close to the serine/water interface and it decreases toward the center of the bulk water. With the aim of studying the tendency of sodium ions to be coordinated by different DPPS oxygens, Figure 6 shows the radial distribution function  $g(r)$  as it was defined in Eq. (1). From the integral of each peak, we obtain the coordination numbers of 0.8, 1.8, and 0.18, for the serine carbonyl, phosphate oxygen, and tail carbonyl oxygens, respectively. Several conclusions can be drawn from these results. The low tendency of the sodium to be coordinated by the tail carbonyl oxygens is a direct consequence of the high tendency of the tail carbonyl to coordi-

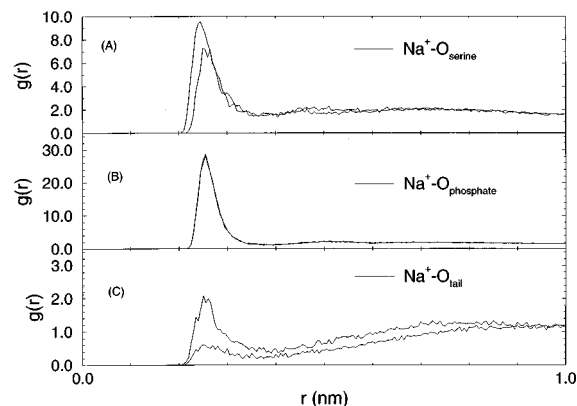


FIG. 6. Radial distribution function of oxygens surrounding sodium ions. (a) Serine oxygens 4,5. (b) Phosphate oxygens 9,10. (c) Carbonyl oxygen tail 16,34.

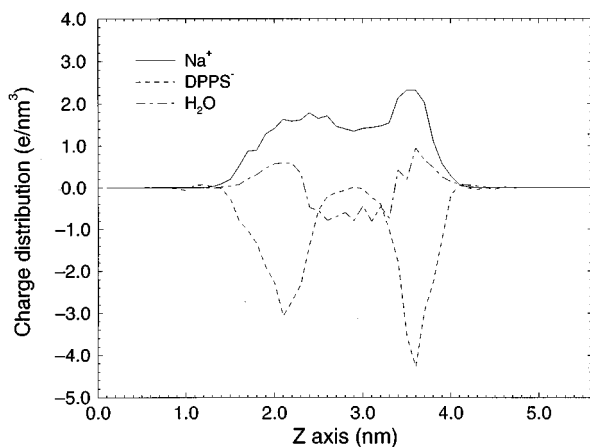


FIG. 7. Atom charge distribution across the membrane.

nate the ammonium groups as we see in Fig. 3(c). Second, an inversion in the coordination numbers between serine and phosphate oxygens is observed compared to their coordination number with ammonium nitrogen. From this, we conclude that the negative charge on serine is mainly compensated by ammonium groups while that for phosphate oxygens is mainly compensated by sodium ions.

In the case of water molecules, the distribution decays from the bulk water to the serine region, as a consequence of the dipolar nature of water, and it vanishes in the hydrocarbon region.

In conclusion, these results show the standard behavior of phospholipid membranes where the phospholipid head groups generate the required electrostatic environment for penetration of water and sodium ions into the membrane, while the hydrocarbon zone is a strong barrier to penetration of charged or polar molecules into the membrane.

Some experimental results on the hydrocarbon thickness of the DPPS have been obtained by  $^2\text{H-NMR}^5$  and by simulation for the DPPC.<sup>18</sup> If we evaluate the membrane thickness from the atom distribution as the distance between the intersection points of the serine and hydrocarbon distributions in both layers, we obtain a thickness of 3.1 nm, which agrees with the experimental value of 3.3 nm of the DPPS at 353 K and the simulation value of 3 nm of the DPPC at 350 K. On the other hand, we see that the thickness of the hydrocarbon interior of the membrane is almost the same as in the DPPC as in DPPC.

Figure 7 displays the charge distribution across the membrane for each of its components. We see that the DPPS charge is mainly neutralized by the sodium ions. The excess of negative charge is further neutralized by water molecules through orientation of their dipole moment. In the bulk of the water layer, the positive charge of the sodium ions is only partially compensated by the orientation of water dipoles. As a consequence of the presence of two sharp peaks for DPPS, the model of a charged condenser with a diffuse double layer<sup>2</sup> for a biological membrane does not differ too much from our simulations. The findings for the neutral DPPC membrane<sup>17</sup> are quite different. A broader and more diffuse

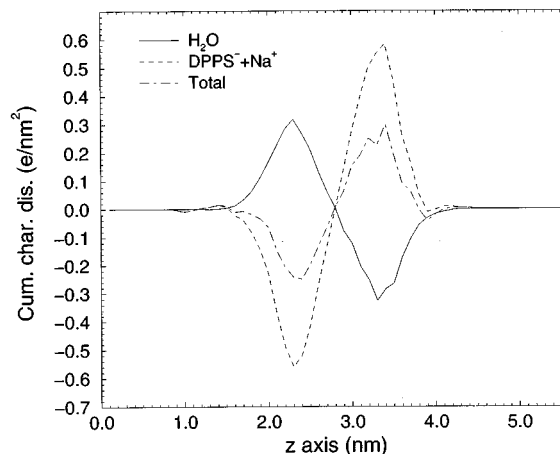


FIG. 8. Cumulative charge distribution across the membrane.

distribution with local charge compensation is obtained.

Another way of displaying the charge distribution within the membrane is through its cumulative charge distribution  $\rho_c(z)$  defined as,

$$\rho_c(z) = \int_0^z \rho(z') dz'. \quad (2)$$

In Fig. 8 we display the cumulative charge distribution for the DPPS+Na<sup>+</sup>, H<sub>2</sub>O, and for all the components together. This figure shows that the water molecules partly compensate the excess of cumulative charge of the DPPS plus Na<sup>+</sup> by orientation of its dipole moment.

The resulting charge density is still appreciable and will lead to a potential difference over the interface. By integrating the cumulative charge distribution once more with respect to  $z$  this potential difference can be computed to be about 2 V.

### C. Order parameters

The deuterium order parameter is a very important information source on the hydrocarbon membrane structure. The order parameter tensor  $S$  is defined by

$$S_{\alpha\beta} = \frac{\langle 3 \cos \theta_\alpha \cos \theta_\beta - \delta_{\alpha\beta} \rangle}{2} \quad \alpha = x, y, z; \beta = x, y, z, \quad (3)$$

where  $\theta_i$  is the angle between the  $i$ th molecular axis and the bilayer normal and  $\delta_{ij}$  is the Kronecker delta. The bilayer axes are defined as follows: The  $z$  molecular axis is the vector perpendicular to the plane which contains the ethylene carbon hydrogens, the  $x$  axis is along the vector which connects both hydrogens and the  $y$  axis is a vector perpendicular to the  $x$  and  $z$  axis. As we do not consider in an explicit way the presence of hydrogens in our simulations (except for the water), the  $z$  axis is defined by the vector which connects the carbons  $C_{i-1}$  and the  $C_{i+1}$ , the  $x$  axis is perpendicular to the  $z$  axis and it is also contained on the plane defined by  $C_{i-1}$ ,  $C_i$ , and  $C_{i+2}$ , and the  $y$  axis is perpendicular to the other two. Experimentally, carbon-deuterium order parameter,  $S_{\text{CD}}$  has been measured by  $^2\text{H-NMR}^5$  of specifically deuter-

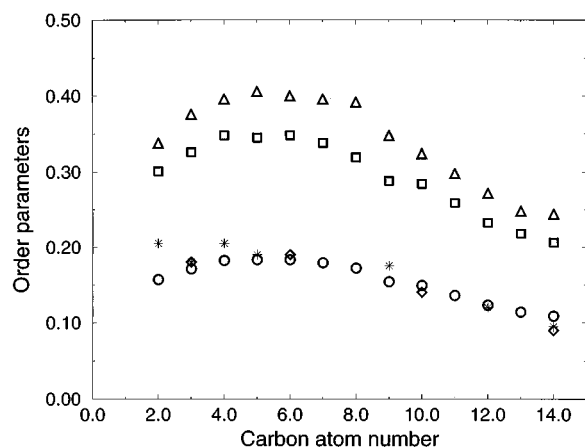


FIG. 9. Order parameters. The first carbon number corresponds to the first atom of the hydrocarbon tail. ( $\square$ )  $S_{zz}$  DPPS simulation; ( $\circ$ )  $-S_{CD}$  DPPS simulation; ( $\triangle$ )  $-2S_{xx}$  DPPS simulation; ( $\diamond$ )  $-S_{CD}$  DPPS experimental (Ref. 5); (\*)  $-S_{CD}$  DPPC experimental (Ref. 33).

ated DPPS along its hydrocarbon chain. The simulation results can be compared with the experimental ones through the relation

$$S_{CD} = \frac{2S_{xx}}{3} + \frac{S_{yy}}{3}, \quad (4)$$

where  $x$  and  $y$  are the molecular axes defined above. In Fig. 9 we show the simulation results and the experimental values for DPPS and DPPC under analogous conditions.<sup>5,33</sup>

If the hydrocarbon phospholipid chains would undergo an isotropic rotation,<sup>34</sup> then  $S_{zz} = -2S_{xx} = -2S_{yy}$ , where  $S_{zz}$  is usually named as  $S_{Chain}$ . Figure 9 shows that  $S_{zz} \neq -2S_{xx}$  and, as a consequence, we conclude that there is rotational anisotropy along the molecular  $z$  axis. This anisotropy results from a correlation between molecular rotation and tilt of the molecules.

We further see that there is a good agreement between experimental and simulation results for DPPS along the chain. We see that  $S_{CD}$  practically remains constant along the central region and decreases toward the end of the hydrocarbon tail. It is also important to note that the order parameters of the first atoms of the DPPS drop remarkably. From a comparison with DPPC, we see that the order parameter profiles are very similar from carbon atom number 6 to the tail end. However, for the first atoms of the tail, we see significant differences of up to 30% between DPPS and DPPC. Obviously, the presence of charge interaction between the  $NH_3$  and the tail carbonyl oxygen is the source of this difference between these phospholipids. As a result of this charge interaction, the  $NH_3$  that belongs to the serine group pulls on the tail carbonyl oxygen and the latter drags the first bonds of the hydrocarbon tail toward a more parallel orientation to the membrane surface. A reduction in the order parameter results, but when leaving the zone of the first atoms, this effect tends to disappear and the situation then approaches the DPPC case.

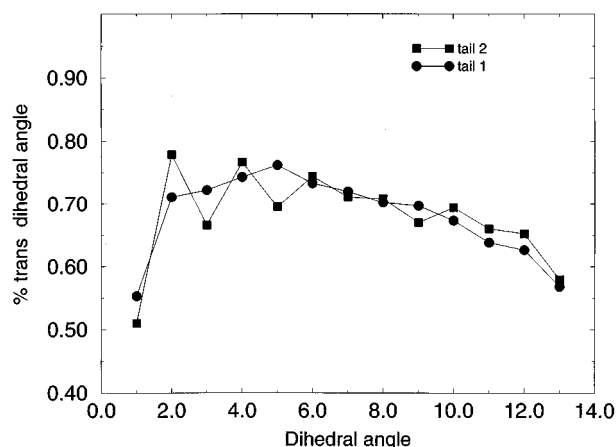


FIG. 10. Dihedral angles statistic for both hydrocarbon tails of the DPPS.

The behavior of the order parameter is reflected in the proportion of trans to cis dihedral angles of the hydrocarbon tails, as is shown in Fig. 10. The fraction of trans never exceeds 75%, as it should be for a liquid crystalline state.

## D. Translational diffusion coefficients

The diffusion coefficients parallel  $D_{t,xy}$  and perpendicular  $D_{t,z}$  to the membrane plane were obtained through the following equations:

$$D_{t,xy} = \frac{1}{4t} \langle (x(t) - x(0))^2 + (y(t) - y(0))^2 \rangle, \quad (5)$$

$$D_{t,z} = \frac{1}{2t} \langle (z(t) - z(0))^2 \rangle, \quad (6)$$

where  $x(0), y(0), z(0)$  and  $x(t), y(t), z(t)$ , are the coordinates of the center of mass at two different times. Then, the diffusion coefficients  $D_{t,xy}$  and  $D_{t,z}$  can be easily obtained in molecular dynamics simulation from the slope of the auto-correlation of mean square displacement.

In the DPPS case, both diffusion coefficients,  $D_{t,xy}$  and  $D_{t,z}$ , were analyzed over two different time scales: a short range of 0–10 ps and a longer range of 0–60 ps. We have to note that the “diffusion constants” evaluated from our simulations (as result of the scale of times that we are employing) reflect more local fluctuations than proper diffusion processes. As consequence, they overestimate the lateral diffusion of lipids and the perpendicular diffusion of lipids is nonexistent. Over a short time range (0–10 ps) the value of the diffusion coefficient measured from our simulations in the plane of the membrane,  $D_{t,xy}^s$  was  $(3.6 \pm 0.3) \times 10^{-6} \text{ cm}^2 \text{ s}^{-1}$ . Unfortunately, no experimental results are available for checking out the validity of our simulations, although some comparisons can be made with results obtained from simulation of DPPC under analogous conditions.<sup>9</sup> In this case a value of  $2 \times 10^{-6} \text{ cm}^2 \text{ s}^{-1}$  was measured at 323 K. For the apparent perpendicular diffusion coefficient,  $D_{t,z}^s$  of the DPPS, a value of  $(7.1 \pm 0.4) \times 10^{-6} \text{ cm}^2 \text{ s}^{-1}$  emerged from our simulations. In this case, a value of  $(10 \pm 1) \times 10^{-6}$

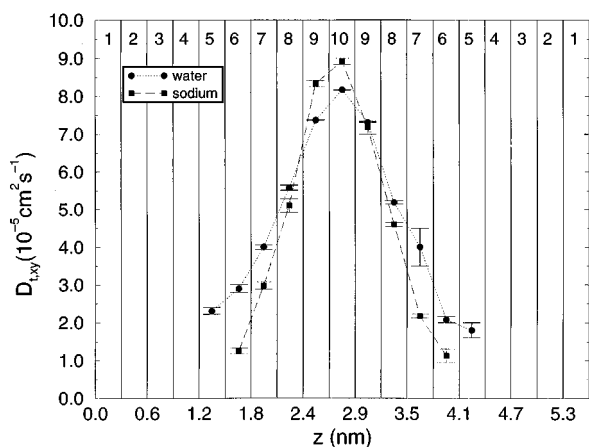


FIG. 11. Diffusion coefficient along the membrane plane, at different depths in the membrane. Slab number 10 corresponds to the bulk of the water layer.

$\text{cm}^2 \text{ s}^{-1}$  was obtained from simulation<sup>35</sup> for a membrane of DPPC at 350 K. In spite of the reasonable agreement with our result, the diffusion coefficient over a short time range is not much smaller than in the DPPC case, as could be expected by the presence of charge interaction between phospholipids. Only a small difference of 40% for DPPS compared to DPPC was found along the perpendicular direction to the membrane plane.

The lateral diffusion coefficient  $D_{t,xy}^l$  over long time range (from 0 to 60 ps), was found to be  $(1.31 \pm 0.02) \times 10^{-6} \text{ cm}^2 \text{ s}^{-1}$  compared to  $5.1 \times 10^{-6} \text{ cm}^2 \text{ s}^{-1}$  obtained from simulations of a DPPC membrane.<sup>18</sup> However, these values are 1 order of magnitude larger than the experimental ones,<sup>36</sup> which typically fall in an order of magnitude between  $10^{-7}$  and  $10^{-8} \text{ cm}^2 \text{ s}^{-1}$ . In the  $D_{t,z}^l$  case, some theoretical and experimental studies of lipid bilayers<sup>37,38</sup> measured values between  $1.3$  and  $2.4 \times 10^{-6} \text{ cm}^2 \text{ s}^{-1}$  in a temperature range from 295 to 353 K, compared to a value of  $(1.6 \pm 0.6) \times 10^{-6} \text{ cm}^2 \text{ s}^{-1}$  from our simulations.

In the water and sodium case, with the aim of obtaining more detailed information about their diffusion coefficient across the membrane, a study along thin slabs at different depths in the membrane was performed, from bulk water to the middle of the membrane. As shown in Fig. 11, the computing box was divided in 10 symmetric slabs of 0.30 nm of thickness each, where the slab numbered 10 just corresponds to bulk water. In this way, we will be able to obtain information about the diffusion of both components at different depths in the membrane. Due to the high mobility of water and sodium ions the particles passed from one slab to another. The trick we used to assign particles to a particular slab was to brake up the trajectory of simulation into several subtrajectories of 10 ps each and assign a molecule during the whole subtrajectory to the slab where its center of mass averaged over the subtrajectory, resides.

From Fig. 11 we observe that the  $D_{t,xy}^s$  decreases from bulk water toward the middle of the membrane. This behavior, shown by both species, is easily understandable as a clear consequence of the Coulombic interaction between

them and the charge of the phospholipid heads. The sodium ions have stronger interactions with the head groups than water and therefore have a more reduced diffusion constant in the head region.

For water, the value of  $(8.170 \pm 0.013) \times 10^{-5} \text{ cm}^2 \text{ s}^{-1}$  for the  $D_{t,xy}$  was measured from our simulations in bulk water (just in slab number 10). This result is in a good agreement with the value of  $7.5 \times 10^{-5} \text{ cm}^2 \text{ s}^{-1}$  measured for the SPC model<sup>39</sup> at 350 K.

Unfortunately, no values are available from our simulations for the diffusion coefficient  $D_{t,xy}^s$  from slabs 1 to 4 (which correspond to the hydrocarbon region of the membrane), because neither water nor sodium penetrated into the membrane beyond slab number 5 during the simulation time. If we wish to evaluate the diffusion coefficient of water or sodium in this zone of the membrane, a different procedure such as the force autocorrelation method<sup>28</sup> should be used. This general method based on the fluctuation–dissipation theorem<sup>40</sup> can be used to study diffusion over free energy barriers.

Comparing the behavior of the diffusion coefficient of water  $D_{t,xy}^s$  in this DPPS membrane with that in a DPPC membrane,<sup>28</sup> we find a very similar behavior in both cases. Only a small difference can be observed in the interface region where in the DPPS membrane the water diffuses faster than in the DPPC membrane.

In the sodium case, a comparison can be made with a system composed of sodium–decanoate/decanol/water<sup>15</sup> at 300 K. If we extrapolate the diffusion coefficient of sodium to a temperature of 350 K, we obtain a value of  $1.5 \times 10^{-5} \text{ cm}^2 \text{ s}^{-1}$ , which falls between the values measured from our simulations of  $1 \times 10^{-5}$  and  $5 \times 10^{-5} \text{ cm}^2 \text{ s}^{-1}$  at the beginning and at the end of the interface, respectively.

## IV. CONCLUSIONS

The DPPS membrane shows some differences in its behavior relative to uncharged phospholipids, in particular DPPC. These differences are mainly caused by charge interactions between adjacent phospholipids.

These charge interactions are so effective that they are able to compensate the high electrostatic repulsions between neighboring phospholipids. They reduce the net surface area per phospholipid around 10% compared to DPPC. Another consequence is the tendency of the phospholipids to cluster which is the cause of the anisotropic distribution of the phospholipid head groups on the membrane plane.

The presence of these charge interactions also results in a more constrained structure of the membrane. The atom distribution across the membrane is rather sharper for the serine group than for the choline group in DPPC and also the charge distribution is sharper than that obtained for a membrane of DPPC. DPPS more closely resembles a model of two charged planes in a condenser. The local charge density is only partially compensated by water and causes an appreciable potential difference over the interface, with the water phase being positive with respect to the membrane interior. Another consequence of the charge interaction between head



groups and tail acyl carbonyl groups, is a reduction in the order parameter of the first atoms of the hydrocarbon tails; this was observed both experimentally and in the simulation.

No significant differences were found between the lateral diffusion constant of DPPS and DPPC. Although the limited length of the simulation does not allow an accurate determination of the diffusion constant, good agreement with experimental values and results of other simulations was found.

The behavior of water also shows some differences compared to water in a DPPC membrane. In DPPS a smaller penetration of the water into the membrane was observed. On the other hand, its lateral diffusion coefficient behaves in a similar way as in the DPPC membrane; it drops from bulk water value to a low value just in the beginning of the hydrocarbon region, inside the membrane. The only difference is that the diffusion coefficient in the DPPS membrane is slightly higher than in the DPPC membrane, which is possibly related to the reduction of the interaction between phospholipids and water.

The interfacial sodium ions appear to be liganded by oxygens of DPPS. As a result of this attachment of sodium to the phospholipids; a reduction in its diffusion coefficient results: The observed diffusion constant for sodium ions was smaller than that found for water, typically a factor of 2 at the deepest zone in the membrane.

## ACKNOWLEDGMENTS

Dr. J.J.L.C. wishes to thank Ministerio de Educación y Ciencia Español his financial support through a Post-Doctoral fellowship, for his research at the University of Groningen, The Netherlands. J.G.T. acknowledges support to Project PB90303 from the same source and project PIB94/07 from the Comunidad Autónoma de la Región de Murcia. This research was supported in part by the Foundation for Biophysics with financial aid from the Netherlands Organization for Scientific Research (NWO).

<sup>1</sup>H. Hauser and G. G. Shipley, *Biochemistry* **22**, 2171 (1983).

<sup>2</sup>G. Cevc and D. Marsh *Phospholipid Bilayers. Physical Principles and Models*, edited by (Wiley, New York, 1987).

<sup>3</sup>R. C. MacDonald, S. A. Simon, and E. Baer, *Biochemistry* **4**, 885 (1993).

<sup>4</sup>H. Hauser, F. Paltauf, and G. G. Shipley, *Biochemistry* **21**, 1061 (1982).

<sup>5</sup>J. L. Browning and J. Seelig, *Biochemistry* **19**, 1262 (1980).

<sup>6</sup>R. W. Pastor, R. M. Venable, and M. Karplus. *J. Chem. Phys.* **89**, 1112 (1988).

<sup>7</sup>H. De Loof, S. C. Harvey, J. P. Segrest, and R. W. Pastor, *Biochemistry* **8**, 2099 (1991).

<sup>8</sup>S. Marčelja, *Biochim. Biophys. Acta* **367**, 165 (1974).

<sup>9</sup>R. M. Venable, Y. Zhang, B. J. Hardy, and R. W. Pastor, *Science* **262**, 223 (1993).

<sup>10</sup>K. V. Damodaran, K. M. Merz, and B. P. Gaber, *Biochemistry* **31**, 7656 (1993).

<sup>11</sup>K. Raghavan, M. R. Reddy, and M. L. Berkowitz, *Langmuir* **8**, 233 (1992).

<sup>12</sup>T. R. Stouch, *Molecular Simulations* **10**, 335 (1993).

<sup>13</sup>H. E. Alper, D. Bassolino-Klimas, and T. R. Stouch, *J. Chem. Phys.* **99**, 5554 (1993).

<sup>14</sup>H. Heller, M. Schaefer, and K. Schulten, *J. Phys. Chem.* **97**, 8343 (1993).

<sup>15</sup>E. Egberts and H. J. C. Berendsen, *J. Chem. Phys.* **89**, 3718 (1988).

<sup>16</sup>H. J. C. Berendsen, B. Egberts, S. J. Marrink, and P. Ahlström, in *Membrane Proteins: Structures, Interactions and Models*, edited by J. Jortner and B. Pullman (Kluwer Academic, Amsterdam, 1992), p. 457.

<sup>17</sup>E. Egberts, Ph.D. Thesis, Rijksuniversiteit, Groningen, The Netherlands, 1988.

<sup>18</sup>E. Egberts, S. J. Marrink, and H. J. C. Berendsen, *Eur. Biophys. J.* **22**, 423 (1994).

<sup>19</sup>HYPERCHEM. Package developed by and licensed from HyperCube, Inc. (1992).

<sup>20</sup>H. J. C. Berendsen, J. P. M. Postma, W. F. van Gunsteren, and J. Hermans, in editor, *Intermolecular Forces*, edited by B. Pullman (Reidel, Dordrecht, 1981), p. 33.

<sup>21</sup>J. A. Pople and G. A. Segal, *J. Chem. Phys.* **44**, 3289 (1966).

<sup>22</sup>B. Jönsson, O. Edholm, and O. Teleman, *J. Chem. Phys.* **85**, 2259 (1986).

<sup>23</sup>H. J. C. Berendsen, J. P. M. Postma, W. F. van Gunsteren, A. DiNola, and J. R. Haak, *J. Chem. Phys.* **8**, 3684 (1984).

<sup>24</sup>G. Cevc, A. Watts, and D. Marsh, *Biochemistry* **20**, 4955 (1981).

<sup>25</sup>W. F. van Gunsteren and H. J. C. Berendsen, GROMOS: GROningen MOlecular Simulation is a software package, Biomos, Nijenborgh 4, 9747AG Groningen, The Netherlands (1987).

<sup>26</sup>W. F. van Gunsteren and H. J. C. Berendsen, *Angew. Chem Int. Ed. Engl.* **29**, 992 (1990).

<sup>27</sup>J. P. Ryckaert and A. Bellemans, *Faraday Discuss. Chem. Soc.* **66**, 95 (1978).

<sup>28</sup>S. J. Marrink and H. J. C. Berendsen, *J. Phys. Chem.* **15**, 4155 (1994).

<sup>29</sup>R. C. MacDonald, S. A. Simon, and E. Baer, *Biochemistry* **4**, 885 (1987).

<sup>30</sup>R. A. Demel, F. Paltauf, and H. Hauser, *Biochemistry* **26**, 8659 (1987).

<sup>31</sup>M. B. Abramson, W. T. Norton, and R. Katzman, *J. Biol. Chem.* **240**, 2389 (1965).

<sup>32</sup>D. Papahadjopoulos and L. Weiss, *Biochim. Biophys. Acta* **183**, 417 (1969).

<sup>33</sup>A. Seelig and J. Seelig, *Biochemistry* **23**, 4839 (1974).

<sup>34</sup>P. van der Ploeg and H. J. C. Berendsen, *J. Chem. Phys.* **76**, 3271 (1982).

<sup>35</sup>S. J. Marrink, M. Berkowitz, and H. J. C. Berendsen. *Langmuir* **11**, 3122 (1993).

<sup>36</sup>*The Structure of Biological Membranes*, edited by Philip Yeagle (CRC, Boca Raton, 1992).

<sup>37</sup>H. Schindler and J. Seelig, *J. Chem. Phys.* **7**, 2946 (1974).

<sup>38</sup>R. T. Roberts, *Nature (London)* **242**, 348 (1973).

<sup>39</sup>J. Postma, Ph.D. thesis, Rijksuniversiteit Groningen, The Netherlands, 1985.

<sup>40</sup>R. Kubo, *Rev. Mod. Phys.* **29**, 255 (1966).